

Calculation of the delayed hydride cracking velocity vs. K_I curve for Zr-2.5 Nb by critical hydride cluster length

D. YAN, R. L. EADIE

Department of Chemical and Materials Engineering, University of Alberta,
Edmonton, Alberta, Canada T6G 2G6
E-mail: reg.eadie@ualberta.ca

In Zr-2.5 Nb alloy the delayed hydride cracking (DHC) velocity versus stress intensity factor K_I relation exhibits a three stage curve. The first two stages of this curve have been numerically simulated by the authors in previous work, using the experimentally measured critical lengths of the hydride cluster for fracture and a numerical analysis of time-dependent hydride growth at the crack tip (D. Yan and R. L. Eadie, *J. Mater. Sci.* **35** (2000) 5667; *Idem.*, *Scripta Mater.* **43** (2000) 89). A modified experimental method was developed and this method allows hydride clusters formed under different K_I to be separated so that the critical hydride length can be measured (Yan and Eadie, 2000). The numerical analysis was based on a simplified model, proposed by Shi and co-workers, that assumes a cylindrically symmetric stress distribution at the crack tip (S. Q. Shi, M. Liao and M. P. Puls, *Modeling Simul. Mater. Sci. Eng.* **2** (1994) 1065; S. Q. Shi and M. P. Puls, *J. Nucl. Mat.* **218** (1995) 30). In this work both the experimental work and the simulation of the DHC velocity versus K_I curve are extended to include a different test temperature and the simulation results are compared with experimental measurements. This result is unique since both velocities and hydride cluster lengths have been determined in the same specimen over the range of K_I right down to K_{IH} . The two temperatures used 150 and 250°C cover the temperature range of most practical interest in CANDU pressure tubes. It was found that the simulated curves were in reasonably good agreement with the experimental measurements. The results also predicted the experimentally observed change in critical hydride length (striation size) with temperature. © 2002 Kluwer Academic Publishers

1. Introduction

Zr-2.5 Nb alloy is a structural material used for manufacturing the pressure tubes of the primary heat transport system in CANDU (Canadian Deuterium Uranium) nuclear reactors. This alloy, despite its excellent combination of mechanical properties, corrosion resistance and low neutron absorption, is susceptible to a fracture mechanism called delayed hydride cracking (DHC). Since the first observation of DHC in Zr-2.5 Nb pressure tubes in the early 1970's, extensive research has been conducted in this area. In general, DHC has been accepted as a repeated process that involves stress-induced hydrogen diffusion, hydride precipitation and hydride fracture [1]. The process usually begins at the tip of preexisting cracks or flaws in the alloys that act as stress raisers. Usually, the stress intensity factor, K_I , is used to characterize the stress state at the crack tip.

The DHC velocity in Zr-2.5 Nb alloy is dependent on K_I , and usually exhibits a three-stage curve, as shown in Fig. 1. In stage I, the DHC velocity is very sensitive to K_I , and increases rapidly with small increases in K_I . There is a threshold value for K_I , i.e. K_{IH} , below which DHC will not occur. In stage II the DHC velocity is

relatively insensitive to K_I and forms a plateau. One characteristic of DHC is that the crack nucleates and propagates for a finite distance in each crack increment [1]. This distance is the hydride length at the crack tip or the striation length shown by fractography. It indicates that the damage zone at the crack tip that is caused by hydride accumulation must grow to a certain length before the crack can propagate. Therefore, it is quite logical that the crack growth rate for DHC is determined by the time for the formation of these damage zones and their lengths.

Recently, the authors performed experimental work [2] to study the critical hydride cluster length at the crack tip for both $K_I < K_{IH}$ and $K_I > K_{IH}$ in the region near K_{IH} . It was proposed that the occurrence of DHC was controlled by two factors: one was the maximum length to which the hydride cluster can grow, and the other was the critical length of hydride cluster required for fracture. Based on these controlling factors, we found that the stage I/II transition in the DHC velocity vs. K_I curve can be explained by the critical lengths of hydride clusters at the crack tip. Furthermore, the DHC velocity vs. K_I curve can be simulated

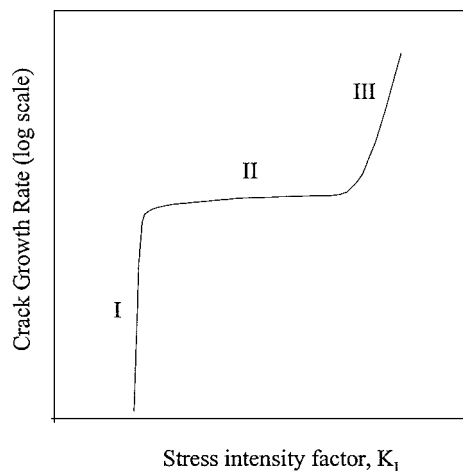


Figure 1 A schematic of the crack growth rate vs. K_I curve for DHC.

by combining the measured critical lengths of the hydride clusters and the calculated times for the hydride growth [3].

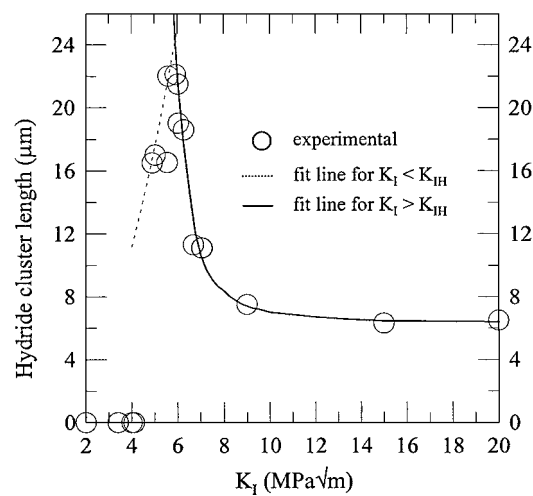
In this work, both the experimental work and the simulation of the DHC velocity vs. K_I curve are extended to include a different test temperature, and the simulation results are compared with experimental measurements. The two test temperatures discussed in this work, 150°C and 250°C, thus cover the temperature range of broadest interest for the application of DHC based on pressure tube operation conditions. The change in critical hydride length with temperature is also examined.

The numerical method used for calculating the time-dependent hydride growth was based on a finite differential analysis and a simplified stress field at the crack tip first proposed by Shi and co-workers [4, 5]. For the experimental part of this work, a series of DHC tests were performed for different K_I , at 150°C and 250°C, respectively. After each experiment, a layer about 0.1 mm thick was ground off one side surface of the specimen. The ground surface was then polished and etched to reveal the hydride clusters formed and fractured along the crack length. Specimens were fatigued between consecutive experiments, so that the crack lengths induced in different experiments were separated and measured [6]. It was found that the simulated results of the DHC velocity vs. K_I curve were in reasonably good agreement with the experimental measurements.

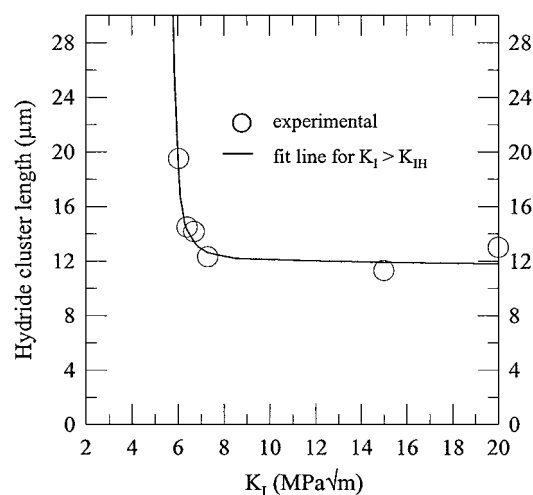
2. Theory

In DHC of the Zr-2.5 Nb alloy, the hydride cluster that forms at the crack tip has a critical length for fracture, which is a function of the stress intensity factor K_I and other material parameters. When $K_I > K_{IH}$, the hydride cluster must grow to this critical length before it will fracture. On the other hand, when $K_I < K_{IH}$, there is a maximum length to which the hydride cluster can grow. This is because the hydride growth is a self-limiting process in this range of K_I , since the driving force (i.e. stress) for hydrogen diffusion decreases as the hydride grows [5]. This maximum length is insufficient for fracture i.e. less than the critical length.

Fig. 2a [2] gives the hydride cluster lengths observed at different K_I at 150°C. The dotted line gives the



(a)



(b)

Figure 2 The hydride cluster length measured at the crack tip as a function of K_I : (a) 150°C and (b) 250°C.

lengths of the single hydride clusters at the crack tip, measured after the specimens were held under load for sufficiently long times. These hydride clusters were not fractured. The solid line gives the lengths of the first hydride clusters at the crack tip, and these hydride clusters were fractured. One sees that as K_I increases, the hydride cluster length first increases for low K_I and then reverses direction when K_I exceeds 6.0 MPa \sqrt{m} . The solid line gives the critical length of the (first) hydride cluster that can be fractured at different applied K_I . The dotted line shows the maximum length to which the hydride cluster can grow. For small K_I this length is insufficient for fracture. The intersection of the dotted and solid lines defines the threshold for DHC. Fig. 2b gives the critical hydride cluster lengths for fracture, i.e. the solid line, at 250°C. Because of some experimental difficulty, the maximum length to which the hydride cluster can grow at 250°C, i.e. the corresponding dotted line for 250°C, could not be measured. This is probably because the density of hydrides in the hydride clusters at 250°C is lower than that in hydride clusters at 150°C, since a hydride cluster consists of both hydrides and matrix ligaments [7–9] and the hydride precipitation is controlled by the peak stress at the crack tip [4, 5]. As a result, the chemical etching to reveal the hydride clusters did not produce sufficient

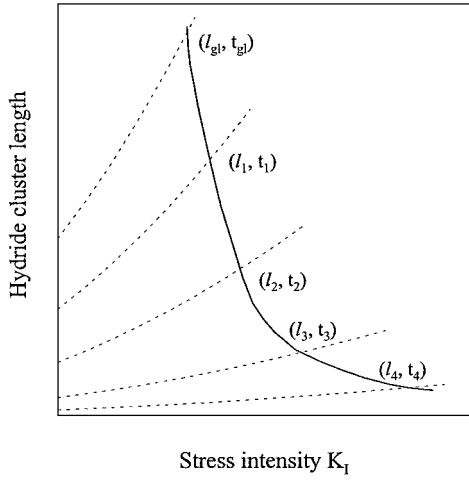


Figure 3 A schematic showing the critical hydride cluster length (solid line) and the lengths of hydride clusters that grow at different diffusion times (dotted lines), as functions of K_I .

contrast. This, however, will not affect the simulation of DHC velocities since only the solid lines in Fig. 2 will be used in the calculation.

The critical length of hydride cluster, as given by the solid lines in Fig. 2, was measured by experiment. The theoretical explanation for this critical hydride length for fracture still remains controversial, due to a lack of clarity in the hydride fracture criteria [5, 10, 11]. However, both of the proposed models, i.e. the critical stress model [5] and the energy balance model [10], predict a curve for critical hydride length similar to the solid lines in Fig. 2. These curves of critical hydride cluster length can be used to calculate the DHC velocity vs. K_I curves, if we consider the time-dependent hydride growth, as shown in Fig. 3. In Fig. 3, the dotted line on the top gives the maximum length to which the hydride cluster can grow for different applied K_I , corresponding to infinitely long diffusion time t_{gl} (here “gl” means “growth limit”). The other dotted lines correspond to hydride cluster lengths at the same K_I 's for smaller diffusion times $t_{gl} > t_1 > t_2 > t_3$ etc. All dotted lines intersect the critical hydride cluster length for fracture (the solid) line at l_{gl} , l_1 , l_2 , and l_3 etc. The DHC velocities at different applied K_I can thus be calculated as $\frac{l_{gl}}{t_{gl}}$, $\frac{l_1}{t_1}$, $\frac{l_2}{t_2}$, and $\frac{l_3}{t_3}$ etc. This schematic will be numerically calculated in the following section.

3. Numerical calculation

Although a precise analysis of the hydrogen diffusion at the crack tip requires finite element analysis tools, a simple and easy-to-handle numerical method using the finite differential method and a cylindrical approximation to the stress field at the crack tip has been developed in [4]. This method gives results that are in reasonable agreement with experiment. This method assumes that the stress field is cylindrically symmetric under plane strain at the crack tip [4, 5] and ignores the change of stress due to hydride formation. Fick's first and second laws for hydrogen diffusion are given according to Equations 1 and 2:

$$J(r, t) = D_H[\nabla C(r, t) - C(r, t)\nabla\Phi(r)], \quad L_h(t) < r < L \quad (1)$$

and

$$\frac{\partial C(r, t)}{\partial t} = \frac{\partial}{\partial r} \left[-\frac{1}{r} J(r, t) \right], \quad L_h(t) < r < L \quad (2)$$

where $J(r, t)$ is the hydrogen flux at distance r from the crack tip at time t ; D_H is the hydrogen diffusivity; $C(r, t)$ is the hydrogen concentration; $\Phi(r) = -\frac{p(r) \cdot V_H}{RT}$ is the hydrostatic stress potential, where $p(r)$ is the hydrostatic stress (positive for tensile stress), V_H the partial molal volume of hydrogen, R the gas constant and T the absolute temperature; $L_h(t)$ is the length of hydride at the crack tip as a function of time, and L is the distance of the boundary used in calculation (about equal to the diffusion distance $\sqrt{D_H t}$). The boundary conditions are given in Equations 3 and 4 as:

$$C(L_h, t) = C_H^P, \quad (3)$$

and

$$J(L, t) = 0, \quad (4)$$

where C_H^P is the hydrogen precipitation *solvus*.

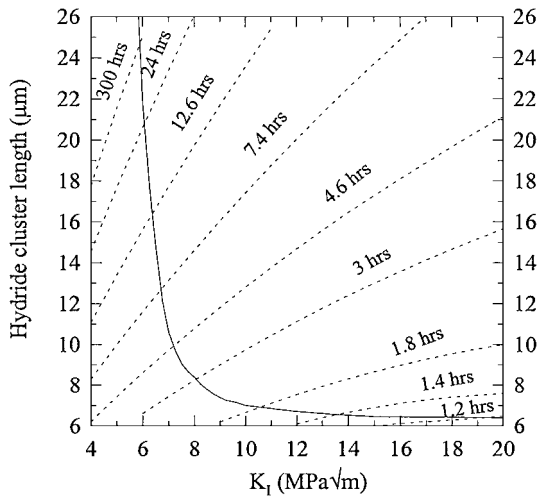
Using this numerical method, we calculated the maximum length to which the hydride cluster can grow at the crack tip and the hydride cluster lengths corresponding to different diffusion times, for 150°C [2] and 250°C, as given by the dotted lines in Fig. 4. In our calculation, the initial hydrogen concentration was assumed to be 96% of the hydrogen precipitation *solvus* at the temperature used. This is to simulate the effect of thermal cycle in which the specimen was heated to a peak temperature about 60°C above the test temperature in order to obtain hydrogen saturation in the specimen [2]. The hydride thickness was assumed to be 3 μm . In real situations, hydride clusters are wedge-shaped [2, 9, 12], and hence the hydride thickness should increase with hydride length, but will be in the range of 2–3 μm for the crack tip stress status and K_I range used in this work. However, the hydride thickness used in the calculation will only slightly affect the resulting overall DHC velocities, but will not affect the shape of the DHC velocity vs. K_I curve. This is because the latter is decided by the critical-hydride-cluster-length curve [3]. The DHC velocities can thus be calculated from the intersections of the dotted lines and the solid lines in Fig. 4 and are given in Fig. 5. The effect of the taper would be to increase the diffusion time as the hydride cluster length curve turns up near a K_I value of 6 or 7 MP a $\sqrt{\text{m}}$. Because those diffusion times are already quite long, the effect is not important.

4. Experimental

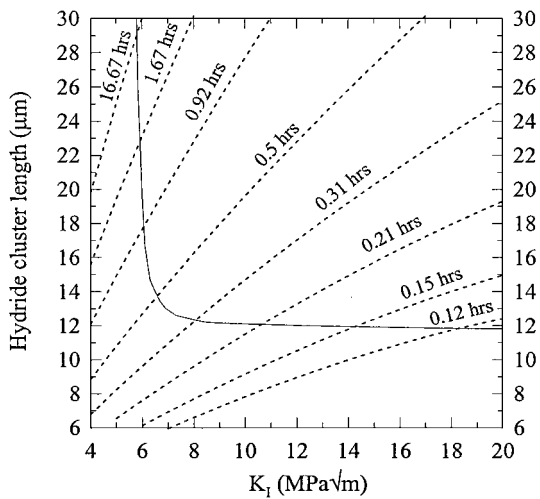
The Zr-2.5 Nb alloy used in this work was provided by the Chalk River Laboratory (CRL) of Atomic Energy of Canada Ltd. (AECL). These samples are from different pressure tubes but have very similar characteristics. The composition is given in Table I. The microstructures of the alloy mainly consisted of α and β phases in the proportion 92% to 8%. The texture of similar pressure tube materials had been measured [13]. The fractions of basal pole normals in radial, circumferential and axial directions for this material were 0.32, 0.62 and 0.06

TABLE I Composition of the Zr-2.5 Nb alloy

	Zr	Nb	Sn	Fe	Cr	Ni	Mo	O ($\mu\text{g/g}$)	H ($\mu\text{g/g}$)
wt%	Balance	2.6	0.0025	0.05	0.01	0.0035	0.0025	1200	5



(a)



(b)

Figure 4 The critical hydride cluster length (solid line) and the lengths of hydride clusters that grow for different diffusion times calculated by numerical methods (dotted lines), as functions of K_I : (a) 150°C and (b) 250°C.

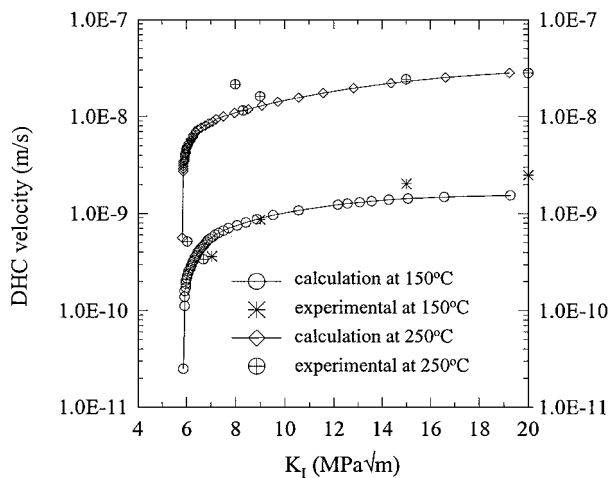


Figure 5 Comparison of the DHC velocity measured by experiment with that calculated by numerical simulation of hydrogen diffusion using the data of the measured critical hydride cluster length.

TABLE II Circumferential tensile properties

Temperature (°C)	Tensile stress (MPa $\sqrt{\text{m}}$)	0.2% yield stress (MPa $\sqrt{\text{m}}$)	Elongation (%)	Area reduction (%)
25	856	826	20	68
150	699	636	20	80
250	650	579	20	81

with only small variations. The circumferential tensile properties were measured, and are given in Table II [14].

Tapered double cantilever beam specimens (constant- K_I specimen) were used for the experiments. In these specimens K_I does not increase with crack length since the stress decreases as the crack gets longer. The specimens were electrolytically hydrided and diffusion-annealed at 400°C, and were then machined by electric discharge machining (EDM). The hydrogen level in the specimens was 165 $\mu\text{g/g}$. The specimens were so cut that the cracking was on the axial-radial plane. To obtain a sharp crack tip, the specimens were fatigue pre-cracked using decreasing ΔK_I . A more detailed description of the preparation is given in [2, 15].

Two testing rigs were simultaneously used for the K_{IH} experiments in this work. Rig 1 was a tension/compression testing machine with the load being computer-controlled through a step-motor. Rig 2 used a lever with a mechanical advantage of 10 to 1 and dead weights for loading. Loading was manual on this rig. Acoustic emission (AE) was the major technique used for monitoring cracking for both rigs, although electrical potential drop (PD) technique was also used in rig 1 [15].

A detailed description of the AE setup is given in [15]. In this work, the AE technique was mainly used to monitor whether cracking had ceased in the specimen. A dummy specimen, which was made of Zr-2.5 Nb alloy, neither pre-cracked nor hydrided, was used to test the noise level of the AE signal collection. As discussed in [2], if no appreciable AE signals were detected, one had reason to believe that all cracking phenomena had ceased in the specimen.

Experiments were performed at both 150°C and 250°C. The temperature was first raised to the peak temperature which was about 60°C above the test temperature, held there for 1 hour (2 hours for rig 2), and then decreased to the testing temperature at a rate of 1–2°C/minute. Then the selected K_I was applied to the specimen. The K_I was kept constant during each experiment. The test time ranged from 40–80 hours. This waiting period was for the hydride cluster at the crack tip to grow to its maximum length or to a length long enough for fracture. When the experiment was finished, the load was first removed and then the specimen was furnace-cooled to room temperature. Between any two

consecutive experiments, the specimen was fatigued to obtain a crack length increment of about $400\ \mu\text{m}$, so that the specimen started with similarly conditioned crack tips for each experiment. After each experiment, a layer of about $0.1\ \text{mm}$ was ground off one side of the specimen and that surface polished and etched to reveal any hydride clusters. This grinding was to remove the plane stress region at the specimen surface [2]. For specimens that had crack propagation, the total crack length was measured, and divided by the total test time under load to obtain the experimentally measured DHC velocity. These DHC velocities are given in Fig. 5.

5. Discussion

Comparing the DHC velocity vs. K_I curve in Fig. 5 with the curve of critical hydride cluster length given in Figs 2 and 4, we can see that the position of the stage I/II transition in DHC velocity vs. K_I curve corresponds to the same K_I as that on the critical hydride cluster length vs. K_I curve. This is the point where the critical length of hydride cluster starts to increase abruptly as K_I decreases. We call this point “the turning point.” This correlation can be explained by using Fig. 4. On the left side of “the turning point”, a small change in K_I results in a relatively small change (1–2 times) in hydride cluster length l_i , but a relatively large change (several orders of magnitude) in diffusion time t_i , since here the diffusion time t_i ranges from several hours to infinity. This is because, as the hydride cluster length approaches the growth limit l_{gl} , the diffusion time t_{gl} required approaches infinity, as shown in Fig. 3. This results in a significant change in DHC velocity, and thus corresponds to stage I. On the right side of “the turning point”, increases in K_I bring about small decreases in both l and t and hence the velocity is nearly constant. Stating it alternatively, both the solid line and the dotted lines tend to be parallel to the K_I axis, and thus the resulting DHC velocities are relatively insensitive to the change of K_I . This is the situation in stage II. Thus we see that the transition between stages I and II of the DHC velocity vs. K_I curve is decided by “the turning point” of the critical hydride cluster length curve, where the critical length of hydride cluster starts to increase abruptly as K_I decreases.

A more accurate definition or the physical meaning of “the turning point” is still not clear. Preliminary study shows that this “turning point” is related to the relative size of the plastic yielding zone at the crack tip to the critical length of hydride cluster for fracture [3].

The calculation results were compared with the DHC velocities measured by experiments using the total crack length divided by the test time. A reasonably good agreement was achieved, as shown in Fig. 5. The analysis predicts (see Fig. 4a and b) that the critical hydride length (striation spacing) should decrease significantly with temperature as was observed experimentally [16]. The decrease in striation length from 250 to 150°C is about a factor of 2, which agrees with the change shown in the experimental curve in reference [16] and

the striation lengths reported in that work were only a bit smaller ($\sim 25\%$) than the cluster sizes measured here. It would not be possible to use those striations in this model, because their variation has not been measured as a function of K_I .

6. Conclusions

1. Based on the experimentally measured critical lengths of hydride cluster for fracture, and a numerical analysis of time-dependent hydride growth at the crack tip, the DHC velocity vs. K_I curve is simulated.

2. The DHC velocities at different K_I can be determined from the intersections between the curve of critical hydride cluster length and the curves of the length of hydride cluster that can grow at the crack tip for different times.

3. The K_I corresponding to the stage I/II transition in the DHC velocity vs. K_I curve corresponds to the K_I where the critical length of hydride cluster for fracture starts to increase abruptly (as K_I decreases), as given in Figs 2 (or 4) and 5.

4. The calculated DHC velocity shows a reasonably good agreement with experimental measurement.

5. The curves predict that the critical hydride length (striation length) should decrease significantly with temperature as is observed experimentally.

Acknowledgments

Funding from NSERC and support from the University of Alberta through a fellowship (D. Yan) are gratefully acknowledged.

References

1. R. DUTTON, K. NUTTALL, M. P. PULS and L. A. SIMPSON, *Metall. Trans.* **8A** (1977) 1553.
2. D. YAN and R. L. EADIE, *J. Mater. Sci.* **35** (2000) 5667.
3. *Idem.*, *Scripta Mater.* **43** (2000) 89.
4. S. Q. SHI, M. LIAO and M. P. PULS, *Modeling Simul. Mater. Sci. Eng.* **2** (1994) 1065.
5. S. Q. SHI and M. P. PULS, *J. Nucl. Mat.* **218** (1995) 30.
6. D. YAN and R. L. EADIE, *Int. J. Press. Vess. Piping* **77** (2000) 167.
7. E. SMITH, *J. Mater. Sci.* **30** (1995) 5910.
8. *Idem.*, *Int. J. Pres. Ves. & Piping* **61** (1995) 1.
9. G. K. SHEK, M. T. JOVANOVIĆ, H. SEAHRA, Y. MA, D. LI and R. L. EADIE, *J. Nucl. Mat.* **231** (1996) 221.
10. X. J. ZHENG, L. LUO, D. R. METZGER and R. G. SAUVE, *ibid.* **218** (1995) 174.
11. X. J. ZHENG, D. R. METZGER, G. GLINKA and R. N. DUBEY, in *ASME PVP Computer Technology: Application and Methodology*, Vol. 326 (1996) p. 181.
12. D. R. METZGER and R. G. SAUVE, in *ASME PVP, Computer Technology: Application and Methodology*, Vol. 326 (1996) p. 137.
13. C. E. COLEMAN, ASTM STP 754 (*ASTM*, Philadelphia, 1982) p. 393.
14. D. YAN and R. L. EADIE, *J. Mater. Sci. Lett.* **19** (2000) 2051.
15. G. LIN, S. SKRZYPEK, D. LI and R. L. EADIE, *J. Testing Evaluation* **26** (1998) 15.
16. L. A. SIMPSON and M. P. PULS, *Met. Trans.* **10A** (1979) 1093.

Received 1 June 2001

and accepted 26 August 2002